



Trade Science Inc.

# Materials Science

An Indian Journal

Full Paper

MSAIJ, 7(1), 2011 [7-11]

## Studies on dielectric and magnetic properties of Co-Ni-Mn ferrite system

K.Y.Rajpure<sup>1\*</sup>, P.K.Chougule<sup>1</sup>, R.C.Kambale<sup>1</sup>, Y.D.Kolekar<sup>2</sup>, C.H.Bhosale<sup>1</sup><sup>1</sup>Composite Materials Laboratory, Department of Physics, Shivaji University, Kolhapur- 416 004, Maharashtra, (INDIA)<sup>2</sup>Department of Physics, University of Pune, Ganeshkhind, Pune- 411 007, Maharashtra, (INDIA)

E-mail : rajpure@yahoo.com

Received: 4<sup>th</sup> August, 2010 ; Accepted: 14<sup>th</sup> August, 2010

### ABSTRACT

The structural, dielectric and magnetic properties of the spinel ferrite system  $\text{Co}_{0.7-x}\text{Ni}_x\text{Mn}_{0.3}\text{Fe}_2\text{O}_4$  ( $x = 0.05, 0.1, 0.15$ ) have been reported. Polycrystalline samples of this series have been prepared by the double sintering ceramic method. The phase identification and structural parameters such as the lattice constant and x-ray density have been determined by using X-ray diffraction technique. An IR studies show the presence of absorption bands at around  $600\text{ cm}^{-1}$  ( $\nu_1$ ) and  $400\text{ cm}^{-1}$  ( $\nu_2$ ); these indicate the presence of tetrahedral and octahedral group complexes, respectively, within the spinel lattice. The dielectric behavior of the system has been studied by measuring the real ( $\epsilon'$ ) dielectric constant in the frequency range 20Hz-1MHz at room temperature. All compositions exhibit normal dielectric dispersion behavior, attributed to Maxwell–Wagner type interfacial polarization mechanism. The room temperature magnetization measurements showed that the saturation magnetization ( $M_s$ ) increases with increase in Ni content, which is an anomalous behavior observed than that of expected. The maximum  $M_s$  of 82 emu/gm is observed for composition  $x = 0.15$  which will be best suitable constituent phase for making the ferrite- ferroelectric magnetoelectric composite materials in future.

© 2011 Trade Science Inc. - INDIA

### INTRODUCTION

The field of ferrites is well cultivated, due to their various potential applications and the interesting physics involved in them. Even after more than half a century, scientists, researchers, technologist and engineers are still interested in various types of ferrite materials, substituted with different cations, prepared by different techniques, and their various properties as a function of composition, temperature, frequency, etc, in bulk, thin film and nanoparticle form. The studies of electric and dielectric behaviour are equally important as those of the magnetic properties, from both the applied and fun-

damental research points of view<sup>[1]</sup>. It is well known that the intrinsic properties of ferrites largely depend on chemical composition and preparation conditions<sup>[2]</sup>. By introducing relatively small amount of divalent metal ions, the structural, magnetic and dielectric properties of ferrites can be modified<sup>[3,4]</sup>. Several researchers have integrated various substitutions and studied the magnetic, dielectric and thermal properties of ferrites, such as Ni-Co<sup>[5-9]</sup>. Further,  $\text{CoFe}_2\text{O}_4$  is being investigated as an alternative ceramic material for developing novel magnetostrictive smart materials<sup>[10]</sup>. It is shown that Mn-substituted Co ferrites are excellent candidates for stress sensors due to a large magnetomechanical effect and

## Full Paper

**TABLE 1 : Structural, Infrared, dielectric and magnetic data of Co-Ni-Mn ferrite system**

Composition (x)	A (Å <sup>2</sup> )	X-ray density Dx (g/cm <sup>3</sup> )	v <sub>1</sub> (cm <sup>-1</sup> )	v <sub>2</sub> (cm <sup>-1</sup> )	Dielectric constant at (1KHz)	Hc (Oe)	Mr (emu/gm)	Ms (emu/gm)
0.05	8.39	5.065	588.12398	13.13	55.39	291.61	15.13	48.67
0.1	3.38	5.079	584.45401	1.84	64.63	211.50	11.29	73.33
0.15	3.38	5.085	591.26412	1.17	66.85	176.26	22.84	81.79

high sensitivity to stress<sup>[11-13]</sup>.

It is reported that the composition  $x \approx 0.3$  of  $\text{Co}_{1-x}\text{Mn}_x\text{Fe}_2\text{O}_4$  is an optimum composition showing a comparatively higher magnetostriction at relatively lower magnetic fields<sup>[15]</sup>. Nowadays a highly magnetostrictive and resistive ferrite phase has become an essential part of ferrite-ferroelectric magnetoelectric (ME) composites which show the magnetoelectric effect<sup>[16,17]</sup>. It has been reported by Devan et al that, in order to obtain a good magnetoelectric response in ME composites, the ferrite phase should be highly magnetostrictive possessing high resistivity<sup>[18]</sup>. Focusing on these objectives, we have prepared the  $\text{Co}_{0.7-x}\text{Ni}_x\text{Mn}_{0.3}\text{Fe}_2\text{O}_4$  ( $x = 0.05, 0.1, 0.15$ ) system and report their structural, magnetic and dielectric properties.

## EXPERIMENTAL

### Sample preparation

All the compositions of  $\text{Co}_{0.7-x}\text{Ni}_x\text{Mn}_{0.3}\text{Fe}_2\text{O}_4$  ( $x = 0.05, 0.1, 0.15$ ) system were prepared by double sintering ceramic method. The AR grade starting materials such as NiO,  $\text{CoCO}_3$ ,  $\text{Mn}_2\text{O}_3$  and  $\text{Fe}_2\text{O}_3$  were taken in the required stoichiometric ratio and milled for 3 hrs. in an agate mortar. The milled powder was pre-sintered at  $1000^\circ\text{C}$  for 4 h in ambient atmosphere. These powders were uniaxially pressed in a die to form pellets (thickness of 2–3mm and diameter of 15mm) using hydraulic press. Polyvinyl alcohol (10% of its weight) was used as a binder during the formation of pellets. The resulting pellets were final sintered at  $1050^\circ\text{C}$  for 4 h. The heating rate of  $1^\circ\text{C}/\text{min}$  and natural cooling was adopted for the both heat treatments.  $\text{Mn}_2\text{O}_3$  formation and presence of  $\text{Mn}^{3+}$  was observed in  $\text{MnFe}_2\text{O}_4$  when heated above  $1050^\circ\text{C}$ <sup>[19]</sup>.

### Characterizations

The confirmation of single-phase formation was car-

ried out by X-ray diffractometer (XRD) (Philips Model PW-3710) using Cr-K $\alpha$  radiation ( $\lambda = 1.54056 \text{ \AA}$ ). For electrical measurements, all the samples were painted on both sides with silver paste to ensure good ohmic contacts. The real ( $\epsilon'$ ) dielectric constant was measured at room temperature as a function of applied frequency range from 100 Hz to 1 MHz by using LCR precision meter (Model HP 4284 A). The real ( $\epsilon'$ ) dielectric constant was calculated by using the relation,

$$\epsilon' = \frac{Cd}{\epsilon_0 A} \quad (1)$$

where, C is the capacitance of the sample, d is the thickness of the sample; A is the cross-sectional area and  $\epsilon_0$  is the permittivity of free space ( $8.854 \times 10^{-14} \text{ F/cm}$ ).

## RESULTS AND DISCUSSION

### X-ray diffraction

X-ray diffraction (XRD) patterns of  $\text{Co}_{0.7-x}\text{Ni}_x\text{Mn}_{0.3}\text{Fe}_2\text{O}_4$  (with  $x = 0.05, 0.1, 0.15$ ) are shown in figure 1. The XRD patterns reveal the polycrystalline nature of the sample with cubic spinel structure, confirmed by analyzing the patterns with JCPDS cards 74-2081, 74-2403 and 22-1086. It observed that, the lattice parameter (a) decreases with increase of Ni content, which is attributed to the replacement of larger ionic radii  $\text{Co}^{2+}$  ions ( $0.78 \text{ \AA}$ ) by smaller ionic radii  $\text{Ni}^{2+}$  ions ( $0.74 \text{ \AA}$ ) and thus obeys the Vegards law<sup>[20,21]</sup>.

Theoretical density was estimated by using the relation<sup>[22]</sup>,

$$D_x = \frac{8M}{Na^3} \quad (2)$$

where M is the molecular weight of ferrite, N is the Avogadro's number and  $a^3$  is the volume of unit cell. It is observed that the X-ray density increases with increase in Ni content. This may be due to the fact that density of pure  $\text{CoFe}_2\text{O}_4$  is ( $5.29 \text{ g/cm}^3$ ) and that of  $\text{NiFe}_2\text{O}_4$  is ( $5.38 \text{ g/cm}^3$ ).

### Infrared (IR) spectroscopy

The IR absorption bands in ferrites ( $\text{MFe}_2\text{O}_4$ ) mainly appear due to the vibrations of oxygen ions with cations. As the concentration of divalent metal ion increases in ferrites, it gives rise to structural change in spinel lattice. Figure 3 shows, the IR absorption bands

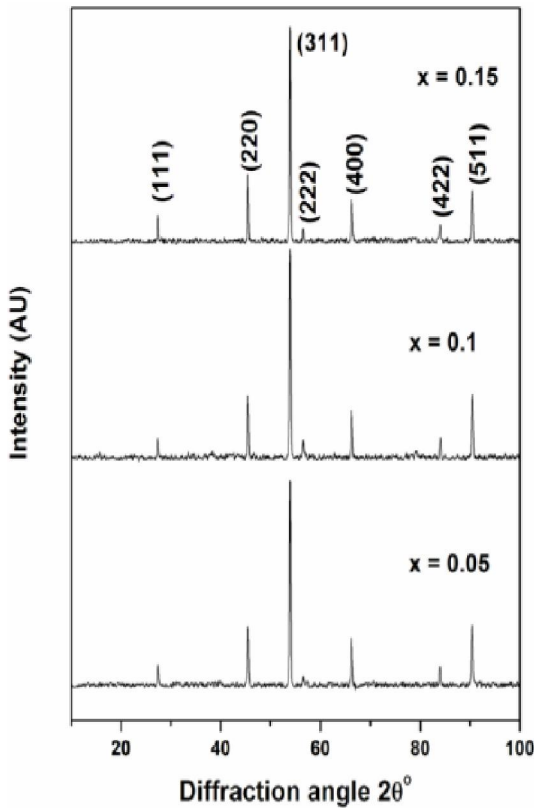


Figure 1 : X-ray diffraction (XRD) patterns of  $\text{Co}_{0.7-x}\text{Ni}_x\text{Mn}_{0.3}\text{Fe}_2\text{O}_4$  system

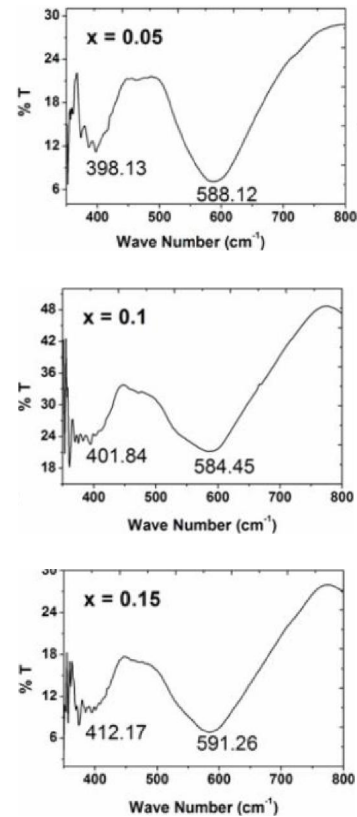


Figure 2 : The IR absorption bands of  $\text{Co}_{0.7-x}\text{Ni}_x\text{Mn}_{0.3}\text{Fe}_2\text{O}_4$  system

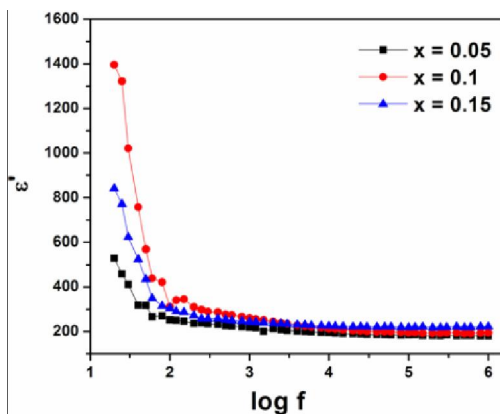


Figure 3 : The frequency dependence of real dielectric constant ( $\epsilon'$ ) of  $\text{Co}_{0.7-x}\text{Ni}_x\text{Mn}_{0.3}\text{Fe}_2\text{O}_4$  system

for  $\text{Co}_{0.7-x}\text{Ni}_x\text{Mn}_{0.3}\text{Fe}_2\text{O}_4$  compositions and the observed values of absorption bands are listed in TABLE 1. It shows that higher absorption bands are in the range from  $584\text{ cm}^{-1}$  to  $591\text{ cm}^{-1}$  and lower absorption bands in the range from  $398\text{ cm}^{-1}$  -  $412\text{ cm}^{-1}$  attributed to the stretching of intrinsic vibrations of the tetrahedral (A) and octahedral (B) sites of spinel lattice respectively. The differences in the band positions for tetrahedral site

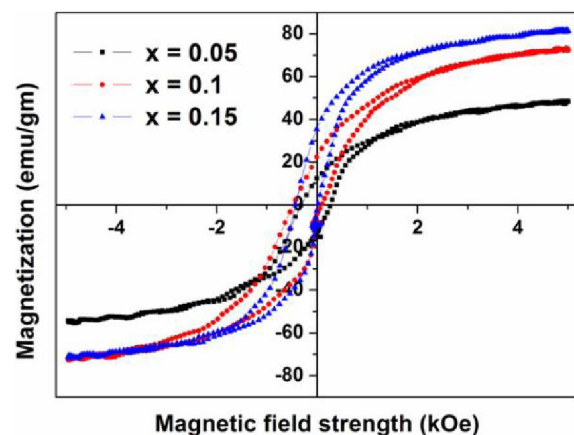


Figure 4 : B-H loops of  $\text{Co}_{0.7-x}\text{Ni}_x\text{Mn}_{0.3}\text{Fe}_2\text{O}_4$  system

( $\nu_T$ ) and octahedral site ( $\nu_O$ ) are expected because of the difference in  $\text{Fe}^{2+}$ - $\text{O}^{2-}$  bond length for the tetrahedral site ( $0.189\text{ nm}$ ) and octahedral site ( $0.199\text{ nm}$ ) of the spinel lattice<sup>[23,24]</sup>. As the vibrational frequency is proportional to the force constant, force constant increases with increase in Ni content for tetrahedral site. The observed values of force constant are given in Table 1. The force constant values are calculated using the

## Full Paper

following relation<sup>[25]</sup>,

$$F_c = 4\pi^2 c^2 v^2 m \quad (3)$$

where  $c$  is velocity of light  $= 2.99 \times 10^{10} \text{ cm sec}^{-1}$   $v$  is the vibrational frequency of tetrahedral and octahedral site of  $\text{Co}_{0.7-x}\text{Ni}_x\text{Mn}_{0.3}\text{Fe}_2\text{O}_4$  and  $m$  is the reduced mass  $= 2.06 \times 10^{-23} \text{ gm}$ .

### Dielectric properties

The frequency dependence of real dielectric constant ( $\epsilon'$ ) for all the samples was studied at room temperature. Figure 4 shows the variation of real dielectric constant with frequency. It is observed that the  $\epsilon'$  sharply decreases at lower frequencies and remain constant at higher frequencies revealing the usual dielectric dispersion behavior attributed to Maxwell–Wagner type interfacial polarization mechanism. The polarizations mainly occur due to, (1) Random distribution of charge carrier densities (space charge polarization). (2) Displacement of positive and negative sublattices under an applied field (ionic polarization). (3) Displacement of negatively charged electron shell against the positively charged core (electronic polarization).

The decrease in permittivity with frequency can be explained on the basis of Koops theory<sup>[26]</sup>, which considers the dielectric structure as an inhomogeneous medium of two layers of the Maxwell–Wagner type<sup>[27]</sup>. In this model, the dielectric structure is assumed to be consisting of well conducting grains which are separated by poorly conducting grain boundaries. It was found that for ferrites, the permittivity is directly proportional to the square root of conductivity<sup>[28]</sup>. Therefore the grains have higher values of conductivity and permittivity, while the grain boundaries have lower values. At lower frequencies the grain boundaries are more effective for conductivity and permittivity than grains. Therefore permittivity is high at lower frequencies and decreases as frequency increases. According to SEM grain size is found to be decreased with increase in Ni content which results into more number of grains and grain boundaries. Thus dielectric constant goes on increasing with increasing Ni content.

### Magnetic properties

Room temperature magnetic hystereses for all the compositions of  $\text{Co}_{0.7-x}\text{Ni}_x\text{Mn}_{0.3}\text{Fe}_2\text{O}_4$  system are shown in figure 5. It is seen that the saturation magneti-

zation  $M_s$  increases with increase of Ni content for Co-Mn ferrite system. Actually, the  $M_s$  has to be decrease with the substitution of  $\text{Ni}^{2+}$  ( $2\mu_B$ ) for  $\text{Co}^{2+}$  ( $3\mu_B$ ), but it is increasing with Ni showing an anomalous magnetic behavior. This incongruity arises mainly due to cation distribution of spinel lattice<sup>[29]</sup>. The increase in saturation magnetization can be well explained with the help of Neel's two sublattice model according to which, saturation magnetization is given by the relation<sup>[30]</sup>,

$$M_s = M_B - M_A \quad (4)$$

where,  $M_B$  and  $M_A$  are the magnetic moments of cations at B-site and A-site respectively. On the basis of this, we can say that magnetic moment of spinel lattice in ferrite is mainly dependent on magnetic ions present at A and B-sites. Assuming  $\text{Co}_{0.7}\text{Mn}_{0.3}\text{Fe}_2\text{O}_4$  as parent ferrite (for  $x = 0.0$ ) addition of Ni ions increases the magnetic moment of B-site as  $\text{Ni}^{2+}$  prefers B-site<sup>[31]</sup>. During high sintering temperature, there is a possibility that Mn can change from  $\text{Mn}^{2+}$  ( $4\mu_B$ ) to  $\text{Mn}^{3+}$  ( $5\mu_B$ ) due to its variable oxidation states and results in higher magnetization. In  $\text{MnFe}_2\text{O}_4$ , 20% of Mn is substituted in octahedral site as  $\text{Mn}^{3+}$  and therefore equivalent amount of Fe will be present as  $\text{Fe}^{2+}$  for charge compensation<sup>[20,32,33]</sup>, thus the random distribution of  $\text{Mn}^{2+}$  and  $\text{Mn}^{3+}$  at A-site and B-site contributes to higher magnetization. Magnetic moments of the formula unit are calculated by using the relation<sup>[2]</sup>,

$$\mu_B = \frac{M \times M_s}{5585} \quad (5)$$

where,  $M$  is the molecular weight of particular composition and  $M_s$  is saturation magnetization (emu/gm).

## CONCLUSION

The  $\text{Co}_{0.7-x}\text{Ni}_x\text{Mn}_{0.3}\text{Fe}_2\text{O}_4$  ( $x = 0.05, 0.1, 0.15$ ) system have been successfully prepared by double sintering ceramic method. The X-ray diffraction technique confirms the phase formation and reveals the spinel cubic structure of the final product. The IR absorption spectra show the presence of two absorption bands in the Co-Ni-Mn ferrite system which confirms the presence of two sublattices (A-site and B-site). The presence of Mn may be responsible for anomalous behavior in magnetic as well as dielectric properties of the Co-Ni-Mn system. All the samples exhibit the dielec-



tric dispersion behavior. The Ms of Co-Mn system increases with the addition of Ni content, maximum Ms of 82 emu/gm is observed for composition  $x = 0.15$  which will be best suitable constituent phase for making the ferrite-ferroelectric magnetoelectric composite materials in future.

## REFERENCES

- [1] N.H.Vasoya, V.K.Lakhani, P.U.Sharma, K.B.Modi, R.Kumar, H.H.Joshi; *J.Phys.*, 8063-8092 (2006).
- [2] P.A.Shaikh, R.C.Kambale, A.V.Rao, Y.D.Kolekar; *J.Magnetism and Magnetic Mater*, **322**, 718-726 (2010).
- [3] S.A.Mazen, H.M.Zaki, S.F.Mansour; *Int.J.Pure and Appl.Phys.*, **3**, 40 (2007).
- [4] S.L.Kadam. C.M.Kanamadi, K.K.Patankar, B.K.Chougule; *Mater.Lett.*, **59**, 215 (2005).
- [5] M.H.Sirvetz, J.H.Saunders; *Phys.Rev.*, **102**, 366 (1956).
- [6] I.P.Kaminow; *J.Appl.Phys.*, **31**, 220 (1960).
- [7] A.E.Paladino, J.S.Waugh, J.J.Green; *J.Appl.Phys.*, **37**, 3371 (1966).
- [8] Q.H.F.Vrehen, B.V.Groenou, A.De, J.G.M.Lau; *Phys.Rev.B*, **1**, 2332 (1970).
- [9] R.C.Kambale, P.A.Shaikh, C.H.Bhosale, K.Y.Rajpure, Y.D.Kolekar; *Smart Mater.Struct.*, **18**, 085014 (2009).
- [10] R.W.McCallum, K.W.Dennis, D.C.Jiles, J.E.Snyder, Y.H.Chen; *Low Temp.Phys.*, **27**, 266 (2001).
- [11] S.S.Shinde, K.M.Jadhav; *J.Mater.Sci.Lett.*, **17**, 849 (1998).
- [12] J.A.Paulsen, C.C.H.Lo, J.E.Snyder, A.P.Ring, L.L.Jones, D.C.Jile; *IEEE Trans.Magn.*, **39**, 3316 (2003).
- [13] J.A.Paulsen, A.P.Ring, C.H.Loc, J.E.Snyder, D.C.Jile; *J.Appl.Phys.*, **97**, 044502 (2005).
- [14] S.D.Bhame, P.A.Joy; *J.Appl.Phys.*, **99**, 073901 (2006).
- [15] S.D.Bhame, P.A.Joy; *J.Phys.D: Appl.Phys.*, **40**, 3263-3267 (2007).
- [16] C.W.Nan, M.I.Bichurin, D.Shuxiang, D.Viehland, G.Srinivasan; *J.Appl.Phys.*, **103**, 031101 (2008).
- [17] S.Priya, R.Islam, D.Shuxianga, D.Viehland; *J.Electroceram.*, **19**, 147 (2007).
- [18] R.S.Devan, C.M.Kanamadi, S.A.Lokare, B.K.Chougule; *Smart Mater.Struct.*, **15**, 1877 (2006).
- [19] S.S.Bhatu, V.K.Lakhani, A.R.Tanna, N.H.Vasoya, J.U.Buch, P.U.Sharma, U.N.Trivedi, H.H.Joshi, K.B.Modi; *Ind.J.Pure Appl.Phys.*, **45**, 596 (2007).
- [20] R.C.Kambale, P.A.Shaikh, N.S.Harale, V.A.Bilur, Y.D.Kolekar, C.H.Bhosale, K.Y.Rajpure; *Journal of Alloys and Compounds*, **490**, 568-571 (2010).
- [21] R.C.Kambale, P.A.Shaikh, S.S.Kamble, Y.D.Kolekar; *Journal of Alloys and Compounds*, **478**, 599-603 (2009).
- [22] J.Smith, H.P.Wijn; *Ferrites*, New York, Wiley, (1959).
- [23] B.Evans, S.Hanfner; *J.Chem.Phy.Sol.*, **29**, 1573 (1968).
- [24] A.Shaikh. S.Jadhav, Watawe, B.Chougule; *Mat.Sci.Let.*, **44**, 192 (2000).
- [25] S.Mazen, A.A.M.R.Nakhla, H.Zaki; *Mat.Chem.Phys.*, **34**, 35 (1993).
- [26] C.G.Koops; *Phys.Rev.*, **83**, 121 (1951).
- [27] K.W.Wagner; *Am.Phys.*, **40**, 317 (1973).
- [28] L.T.Rabinkin, Z.I.Novikova; *Ferrites*, **146**, I2V (1960).
- [29] O.Caltun, H.Chiriac, N.Lupu, I.Dumitru, B.P.Rao, *J.Optoelec; Adv.Mat.*, **9**, 1158 (2007).
- [30] S.Singhal, K.Chandra; *J.Solid State Chem.*, **180**, 296 (2007).
- [31] B.Vishwanathan, V.R.K.Murthy; 'Ferrite Materials Science and Technology', Narosa Pub., House, New Delhi, (1990).
- [32] G.A.Sawatzky, W.F.Van Der, A.H.Morrish; *J.Appl.Phys.*, **39**, 1204 (1968).
- [33] D.Shekhar, Bhame, P.A.Joy; *J.Appl.Phys.*, **100**, 113911 (2006).